AIAA JOURNAL
Vol. 39, No. 10, October 2001

Technical Notes

TECHNICAL NOTES are short manuscripts describing new developments or important results of a preliminary nature. These Notes cannot exceed six manuscript pages and three figures; a page of text may be substituted for a figure and vice versa. After informal review by the editors, they may be published within a few months of the date of receipt. Style requirements are the same as for regular contributions (see inside back cover).

Jet Noise Computations Using Explicit MacCormack Schemes and Nonreflecting Boundary Conditions

Farouk Owis* and P. Balakumar†
Old Dominion University, Norfolk, Virginia 23529

Introduction

DEVELOPING suppression methods for the jet noise relies on accurate computations of the sound radiated from the turbulent mixing layer. The aim of this study is to develop an efficient numerical tool with nonreflecting boundary conditions to evaluate the near-field source of the jet noise and portion of the acoustic field using the direct numerical simulation of Navier–Stokes equations. Recently, many high-order accurate finite difference schemes have been suggested for computational aeroacoustics. Three different categories of numerical schemes have been proposed for computational aeroacoustics. These categories include explicit MacCormack schemes with operator splitting (see Ref. 1), compact finite difference schemes proposed by Lele,[2] and the dispersion-relation-preserving scheme developed by Tam and Webb.[3]

The explicit MacCormack schemes with operator splitting are an extension of the two–four dissipative scheme developed by Gottlieb and Turkel,[4] which is fourth-order accurate in space and second-order accurate in time. The two–four scheme itself is an extension to the second-order MacCormack scheme. One-sided differences are used in the explicit MacCormack schemes to add dissipation for the numerical stability. The accuracy of these schemes is improved by Hixon[1] by adding one point on the opposite side to each of the one-sided differences. Thus, the dispersion and dissipation errors are minimized for each one-sided difference. The new family of MacCormack schemes is tested on benchmark problems. In this work, these schemes are used to study the nonlinear instability of subsonic jets using the unsteady compressible Navier–Stokes equations. Moreover, the numerical boundaries can generate spurious waves that may render the computed solution entirely unacceptable. Several boundary conditions have recently been proposed for computational aeroacoustics. These boundary conditions include characteristic methods,[5] asymptotic analysis of the governing equations,[6] buffer domain technique,[7] and matching layer.[8]

Numerical Method and Results

The governing equations are the unsteady compressible Navier–Stokes equations, which are used in conservative form and cylindrical coordinates. The governing equations can be written in the following vector form:

$$\frac{\partial \boldsymbol{Q}}{\partial t} + \frac{\partial \boldsymbol{F}}{\partial x} + \frac{1}{r}\frac{\partial (r\boldsymbol{G})}{\partial r} = S \tag{1}$$

Received 3 September 1999; revision received 14 March 2001; accepted for publication 8 June 2001.

*Research Associate, Aerospace Engineering Department. Member AIAA.
†Associate Professor, Aerospace Engineering Department. Member AIAA.

High-order-accurate MacCormack-type schemes with operator splitting (see Ref. 1), up to sixth-order accurate in space and fourth-order accurate in time, are used to discretize Eq. (1). The operators are alternated with symmetrical variants such that the schemes maintain their accuracy as explained by Mankbadi et al.[9] and Owis and Balakumar.[10]

The treatment of the boundaries is essential for the jet noise computations. Different boundary conditions are tested here for subsonic jet simulations. At the inflow boundary, nonreflecting boundary conditions are used. These boundary conditions are based on specifying the incoming and the outgoing characteristic waves. At the outflow and radiation boundaries, three different boundary conditions are considered. These boundary conditions are the characteristic boundary conditions, buffer domain, and perfectly matching layer. For the characteristic boundary conditions, all of the incoming characteristics are set equal to zero, and the outgoing characteristics are calculated from the interior points. The buffer domain technique is proposed by Streett and Macaraeg.[7] The technique is based on gradually reducing the ellipticity of the Navier–Stokes equation. The sources of the ellipticity in the equations are smoothly reduced to zero through multiplication by an attenuation function. The perfectly matching layer is applied by Hu[8] for Euler equations. In this technique, a region is attached to the computational domain at the boundaries where exponential damping terms are added to the governing equations to damp the disturbance.

The growth of the instability waves is computed for a high-Reynolds-number supersonic jet to evaluate the explicit MacCormack schemes. A comparison between MacCormack schemes is presented for a different number of points per wavelength. A two-dimensional axisymmetric jet with supersonic Mach number ($M_j = 1.5$) and high Reynolds number ($Re = 1.27 \times 10^6$) is considered for the comparison. We found that the optimized dispersion-relation-preserving (DRP) scheme produced minimum dispersion and dissipation errors compared with all other explicit MacCormack schemes. Even after reducing the grid size in the axial direction from 17 points per wavelength to 9, the results produced by the DRP scheme is not much affected. As the grid size in the axial direction is reduced to 9 points per wavelength, the two–four scheme has high dispersion error compared with the DRP scheme as shown in Fig. 1a. The results indicate that higher growth rate is obtained for the two–four scheme, although this scheme should have higher dissipation error. Using a coarse grid introduces a numerical disturbance, which grows due to the flow instability and, hence, higher wave amplitude is obtained. A comparison between the two–six scheme and the dispersion-preserving scheme is introduced in Fig. 1b. The results indicate that the dispersion error for the two–six scheme with the coarse grid is lower than that of the two–four scheme with the same grid size and that the amplitude of the axial velocity disturbance is relatively higher than that of the dispersion-preserving scheme for the fine grid. However, the two–six and four–six schemes are much better than the two–four scheme; the best results are predicted with the optimized dispersion-preserving scheme. The results of the boundary treatments for the jet problem are introduced in Figs. 2 and 3. Different boundary conditions such as characteristic boundary conditions, buffer domain method, and perfectly matching layer technique are compared with a reference solution obtained from long-domain simulation. A subsonic cold jet with $M_j = 0.85$ and Reynolds number 2500 is considered for the comparisons. The computational domain of interest is extended to 50 radii in the axial direction and 15 radii in the radial direction with grid dimensions of

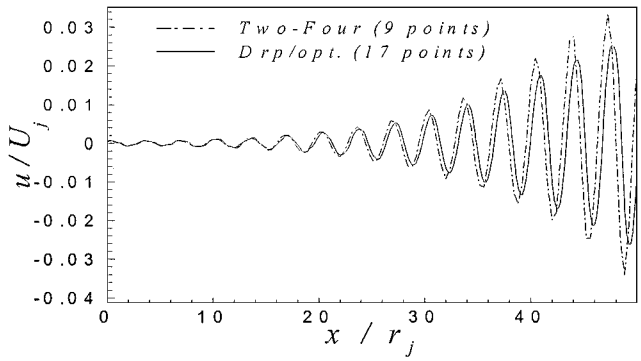

a) 2–4 and DRP schemes

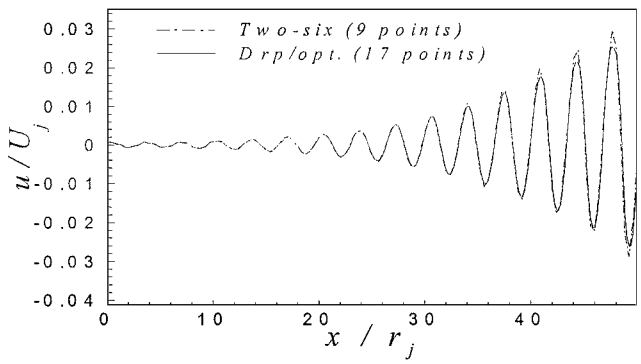

b) 2–6 and DRP schemes

Fig. 1 Axial velocity disturbance vs axial distance for different grid size, $M_j = 1.5$ and $Re = 1.27 \times 10^6$.

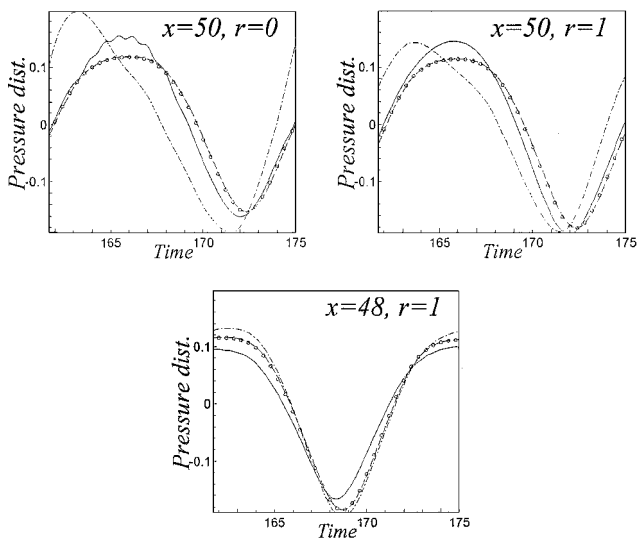

Fig. 2 Time history of the pressure disturbance for one periodic cycle (——, buffer domain; □, long domain; - - -, characteristic boundary conditions; and - - - -, matching layer).

500×200 points. A uniform grid is used in the axial direction, and the grid is clustered in the radial direction at $r = 1$ with clustering parameter 4.5. For the perfectly matching layer technique, a layer of 7 radius length and of 70 grid points is attached close to the outflow boundary at the downstream location. Another layer with the same thickness is added at the radiation boundary, and 30 grid points are used for this layer. A buffer domain with 12 radius thickness and 120 points is used in the axial direction. The time signal of the pressure disturbances at different positions in the computational domain is presented in Fig. 2 for different boundary conditions. The results indicate that maximum wave reflections are caused by the characteristic boundary conditions. As a result of the characteristic boundary treatment, the phase and amplitude of the pressure disturbances are completely different from those of the long-domain simulation. The

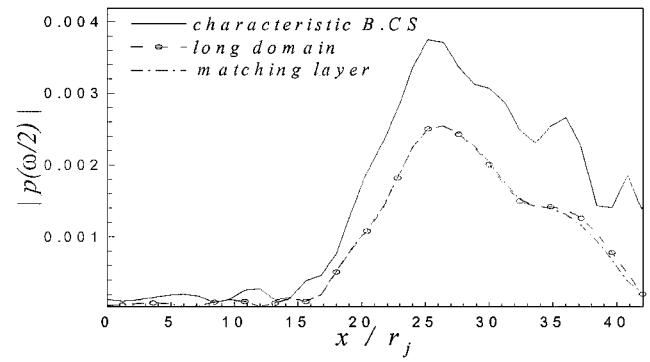

a) $r = 7.5$

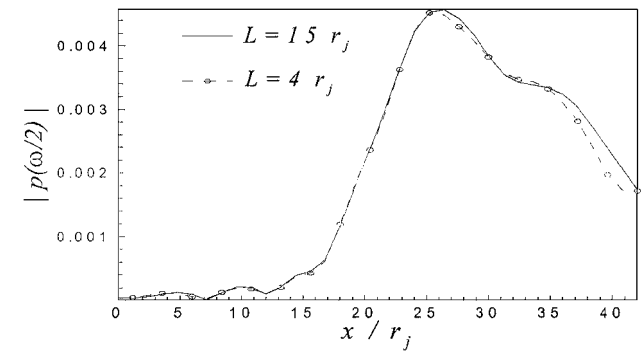

b) $r = 6$

Fig. 3 Amplitude of the pressure disturbance vs axial distance for different lengths of matching layers.

buffer domain technique caused some changes of the predicted disturbance amplitude but the results are still better than those predicted by the characteristic boundary conditions. Minimum reflections are caused by the matching layer technique at the outflow boundaries. The results obtained by the perfectly matching layer are in excellent agreement with the reference solution for the whole computational domain, as shown in Fig. 3a. The variation of the pressure disturbance amplitude with the axial distance for the first subharmonic ($\omega/2$) is introduced in Fig. 3a.

It is clear from Fig. 3 that minimum reflections are caused by the matching layer technique whereas the characteristic boundary conditions render the solution completely different from the reference solution. Thus, the matching layer technique is the kind of boundary treatment that one might rely on for the jet noise simulations because it is not as computationally expensive as the buffer domain technique, and it is nearly perfect for the outflow boundary treatments. Decreasing the length of the perfectly matching layer might causes some reflections at the outflow boundary. To determine the length of the matching layer required for minimum wave reflections, a comparison between two matching layer results with different lengths is shown in Fig. 3b. Two jet simulations are done to calculate the variation of the pressure disturbance amplitude with the axial distance. The first simulation is done with a layer of 15 radius length in the axial direction and the second simulation is computed for a layer of 4 radius length. The same absorption coefficients are used for both layers. The results indicate that some reflections are caused by the shorter layer specially near the outflow boundary. However, the wave reflections are still very small, and the amount of wave reflection does not exceed 2% of the pressure disturbance amplitude.

Conclusions

A numerical method is developed to compute the jet noise using the explicit MacCormack schemes and nonreflecting boundary conditions. The computations indicate that the optimized dispersion-relation-preserving scheme produces minimum dispersion and dissipation errors compared with all other explicit MacCormack schemes. In addition, the results indicate that the perfectly matching layer technique gives minimum reflections at the outflow boundaries. Therefore, the perfectly matching layer technique is suitable for the jet noise simulations.

References

[1]Hixon, R., "On Increasing the Accuracy of MacCormack Schemes for Aeroacoustic Applications," AIAA Paper 97-1586, 1997.

[2]Lele, S. K., "Compact Finite Difference Schemes with Spectral Like Resolution," *Journal of Computational Physics*, Vol. 103, 1992, pp. 16–42.

[3]Tam, C. K. W., and Webb, J. C., "Dispersion Relation Preserving Schemes for Computational Acoustics," *Journal of Computational Physics*, Vol. 107, No. 2, 1993, pp. 262–281.

[4]Gottlieb, D., and Turkel, E., "Dissipative Two-Four Method for Time Dependent Problems," *Mathematics of Computations*, Vol. 30, No. 136, 1976, pp. 703–723.

[5]Thompson, K. W., "Time-Dependent Boundary Conditions for Hyperbolic Systems," *Journal of Computational Physics*, Vol. 68, No. 1, 1987, pp. 1–24.

[6]Bayliss, A., and Turkel, E., "Far Field Boundary Conditions for Compressible Flows," *Journal of Computational Physics*, Vol. 48, Nov. 1982, pp. 182–199.

[7]Streett, C. L., and Macaraeg, M. G., "Spectral Multi-Domain for Large Scale Fluid Dynamics Simulations," *International Journal for Applied Numerical Mathematics*, Vol. 6, 1989, pp. 123–139.

[8]Hu, F. Q., "On Absorbing Boundary Conditions for Linearized Euler Equations by a Perfectly Matching Layer," Inst. for Computer Applications in Science and Engineering, ICASE Rept. 95-70, Hampton, VA, 1995.

[9]Mankbadi, R. R., Hayder, M. E., and Povinelli, L. A., "Structure of Supersonic Jet Flow and Its Radiated Sound," *AIAA Journal*, Vol. 32, No. 5, 1994, pp. 897–906.

[10]Owis, F., and Balakumar, P., "Evaluation of Boundary Conditions and Numerical Schemes for Jet Noise Computations," AIAA Paper 2000-0920, Jan. 2000.

P. J. Morris
Associate Editor

Compressible Dynamic Stall Control Using Dynamic Shape Adaptation

M. S. Chandrasekhara*
Naval Postgraduate School, Monterey, California 93943
and
M. C. Wilder† and L. W. Carr‡
NASA Ames Research Center, Moffett Field, California 94035

Nomenclature

C_p	=	pressure coefficient
$C_{p_{\min}}$	=	peak suction pressure coefficient
c	=	airfoil chord
f	=	frequency of oscillation, Hz
k	=	reduced frequency, $\pi f c/U_\infty$
M	=	freestream Mach number
p	=	static pressure
s, n	=	coordinates along and normal to airfoil surface
x, y	=	chordwise and vertical distance
α	=	angle of attack
α_0	=	mean angle of attack
Ω	=	spanwise component of vorticity

I. Introduction

IT was shown in earlier work[1] on unsteady separation control that changing the leading edge curvature of an NACA 0012 airfoil was effective in producing significant stall delay (about 5 deg at $M = 0.3$) through decreasing leading-edge flow acceleration. The extreme sensitivity of the airfoil peak suction pressure to the flow acceleration around the airfoil leading edge resulted in reduced peak suction levels when the nose radius was increased. Rounding the leading edge also distributed the low-pressure region over a wider extent on the airfoil upper surface, reducing the leading-edge adverse pressure gradient, thus making it possible for the airfoil to reach higher angles of attack before stalling, in both steady and unsteady flows. As a result, satisfactory airfoil performance ensued over a larger operating envelope. In Ref. 1, certain intermediate shapes are identified that were dynamic stall vortex free. The redistribution of the vorticity flux arising from tailoring the nose radius can eliminate the dynamic stall vortex completely and vastly improve a pitching airfoil force and moment loops. Thus, such a flow control method is very valuable for compressible dynamic stall control, which is always a leading-edge type of stall, dominated by a strong clockwise vortex convecting over the airfoil.

Although in Ref. 1 control of compressible dynamic stall using fixed, round nosed airfoils was demonstrated, rotor applications require dynamic airfoil shape adaptation because of the large differences in flow speeds on the advancing and retreating sides. Furthermore, the U.S. Army has stipulated that the next generation of helicopters be significantly more capable in terms of load capacity and maneuverability. This requires removing the constraints imposed by the onset of dynamic stall to enlarge the flight envelope. One way a given rotor blade can deliver improved performance is if the potential flowfield over it is suitably altered, so that it can respond to the rapidly changing flow conditions as it flies through a cycle. It is proposed here to use dynamic shape adaptation as a means to achieve this and to avoid compressible dynamic stall on its retreating side. Proper blade adaptation requires determining the shapes that the airfoil can take without stalling during such a maneuver. These shapes depend on the conditions encountered by the rotor blade. To satisfactorily employ this technique, the fluid mechanics of the flow over airfoils of different shapes need to be understood, and have been discussed in Ref. 1.

The present experiments were focused on controlling the flow over a sinusoidally oscillating airfoil by determining the dynamic shape variations that produced the right nose curvature at each instantaneous flow condition, thus producing the most attached flow over the range of angles of attack of interest. A sharp-to-round shape change profile was chosen, while always maintaining the airfoil shapes within the range of a previously determined attached flow envelope,[1] to achieve the desired flow control effect.

II. Description of the Experiment

Practical implementation of real-time adaptation of an oscillating airfoil requires overcoming the demanding challenges of design and fabrication. A NACA 0012 derivative airfoil, known as the dynamically deforming leading edge (DDLE) airfoil, with 15.24-cm chord was specially developed for the present purpose. Its leading 20% is cast from a carbon–fiber composite; the rest is machined from solid metal. The composite fiber is about 50 μm thick at the leading edge and is attached with a tang to a mandrel, shaped to the NACA 0012 profile, housed inside the airfoil. The mandrel, driven by brushless servomotors, translates in the chordwise direction by less than 2 mm to produce up to 320% continuous change in the airfoil leading-edge radius. For convenience, the various shapes used are denoted by integers, with 75-μm mandrel displacement for each shape number change. Shape 0 corresponds to the NACA 0012 profile. More details about the DDLE airfoil design may be found in Ref. 2.

A typical deformation schedule consists of rounding the nose by retracting the leading edge, holding the final shape for a dwell period, and extending the leading edge back to the original shape. As stated earlier, prior studies[1] identified dynamic stall vortex-free geometries, based on which oscillating airfoil shape-change schedules that offered the most potential for success were determined. Two shape-change schedules, one fast and the other slow, along with the corresponding angle-of-attack variations, shown in Fig. 1, were used in this study (for details, see Ref. 3). The oscillations in

Received 14 July 1999; revision received 26 February 2001; accepted for publication 18 June 2001.

*Research Professor and Associate Director, Navy–NASA Joint Institute of Aeronautics, Department of Aeronautics and Astronautics; mailing address: NASA Ames Research Center, M.S. 260-1, Moffett Field, CA 94035-1000. Associate Fellow AIAA.

†Research Scientist, Reactive Flow Environments Branch. Member AIAA.

‡Emeritus Scientist, Aeroflightdynamics Directorate, U.S. Army Aviation and Missile Command and Experimental Physics Branch. Senior Member AIAA.